

Sensitivity to the Higgs Sector of SUSY-Seesaw Models in the Lepton Flavour Violating $\tau \rightarrow \mu f_0(980)$ decay

M. J. Herrero^a, J. Portolés^b and A. M. Rodríguez-Sánchez^a

^a*Departamento de Física Teórica and Instituto de Física Teórica, IFT-UAM/CSIC
Universidad Autónoma de Madrid, Cantoblanco, E-28049 Madrid, Spain*

^b*IFIC, Universitat de València - CSIC, Apt. Correus 22085, E-46071 València, Spain*

Abstract

In this work we study the Lepton Flavour Violating semileptonic $\tau \rightarrow \mu f_0(980)$ decay within the context of SUSY-Seesaw Models, where the MSSM spectrum is extended by three right handed neutrinos and their SUSY partners, and where the seesaw mechanism is used to generate the neutrino masses. We estimate its decay rate when it proceeds via the Higgs mediated channel $\tau \rightarrow \mu H^* \rightarrow \mu f_0(980)$, where H refers to the CP-even MSSM Higgs bosons h^0 and H^0 , and the Lepton Flavour Violating $\tau\mu H$ vertex is radiatively generated via SUSY loops. In order to describe the $f_0(980)$ meson we follow the guidelines from chiral constraints. As an implication of our computation, we explore the sensitivity to the Higgs sector in this decay and compare it with other LFV tau decay channels. The confrontation of our predictions for $\text{BR}(\tau \rightarrow \mu f_0(980))$ with its very competitive present experimental bound leads us to extract some interesting restrictions on the most relevant model parameters, particularly, $\tan \beta$ and m_{H^0} .

1 Introduction

The study of Lepton Flavour Violating (LFV) processes provides one of the most efficient indirect tests of supersymmetric (SUSY) extensions of the Standard Model of Particle Physics [1–6]. The reason is because in SUSY models the lepton and slepton mass matrices are not diagonal in flavour simultaneously, and this misalignment leads to intergenerational interactions between leptons and sleptons with neutralinos and charginos at tree level, that when placed into the loops of lepton flavour changing processes, can generate large rates. Furthermore, in the case of SUSY-Seesaw models, with extended lepton and slepton sectors by three right handed neutrinos, ν_R , and their SUSY partners, $\tilde{\nu}_R$, and where the seesaw mechanism is used to generate the neutrino masses (i.e., the so called Seesaw models of type I [7]), the size of the off-diagonal (in flavour) slepton mass matrix elements that are responsible for LFV, is governed by the strength of the neutrino Yukawa couplings which can be $Y_\nu \sim \mathcal{O}(1)$ or even larger for heavy $M_{\nu_R} \sim 10^{14} - 10^{15}$ GeV. Thus, an interesting connection between neutrino and LFV physics follows, because the large Yukawa couplings of the Majorana neutrinos induce, via loops of SUSY particles, important contributions to LFV processes. In fact, these contributions are in some cases [1–6, 8–23], at the reach of the present experimental sensitivity [24].

The LFV process that is the most sensitive to the neutrino Yukawa couplings, in the SUSY-Seesaw context, is $\mu \rightarrow e\gamma$, where the present experimental sensitivity is at 1.2×10^{-11} [25, 26]. Also $\mu - e$ conversion in heavy nuclei, with present bounds at $\text{CR}(\mu - e, \text{Ti}) < 4.3 \times 10^{-12}$ [27] and $\text{CR}(\mu - e, \text{Au}) < 7 \times 10^{-13}$ [28], and $\mu \rightarrow 3e$ with $\text{BR}(\mu \rightarrow 3e) < 1.0 \times 10^{-12}$ [29], are quite sensitive to LFV in the $\mu - e$ sector. The most competitive LFV process in the $\tau - \mu$ sector is $\tau \rightarrow \mu\gamma$, whose upper bound is now set to 1.6×10^{-8} [30–33]. Moreover, the sensitivity to LFV in $\tau \rightarrow 3\mu$ has improved remarkably in the last years. The present upper bounds from BELLE and BABAR collaborations are 3.2×10^{-8} and 5.3×10^{-8} , respectively [34, 35]. In the last years, several interesting bounds at the 10^{-8} level for some LFV semileptonic tau decays have also been provided [36–39].

In this work, we study the LFV semileptonic tau decay channel $\tau \rightarrow \mu f_0(980)$, which is competitive with other LFV tau decays due to the recently reported bound by BELLE collaboration [40], $\text{BR}(\tau \rightarrow \mu f_0(980)) \times \text{BR}(f_0(980) \rightarrow \pi^+\pi^-) < 3.4 \times 10^{-8}$. In fact, it is at present, the best bound in semileptonic LFV tau decays, improving the other present competitive bound of $\text{BR}(\tau \rightarrow \mu\eta) < 5 \times 10^{-8}$ [33]. The advantage of $\tau \rightarrow \mu\eta$ [9, 13, 21] and $\tau \rightarrow \mu f_0(980)$ [18] over the $\tau \rightarrow \mu\gamma$ channel is their potential sensitivity to the Higgs sector. Whereas the $\tau \rightarrow \mu\eta$ can be mediated by a Z boson and a CP-odd Higgs boson

A^0 , and is dominated by the A^0 just at large $\tan\beta \gtrsim 20$ [21, 23], the $\tau \rightarrow \mu f_0(980)$ decay is exclusively mediated by the exchange of the neutral CP-even Higgs bosons H^0 and h^0 . Therefore, through the $\tau \rightarrow \mu f_0(980)$ channel one is testing directly the neutral CP-even Higgs sector at all $\tan\beta$ values.

Our computation of the $\text{BR}(\tau \rightarrow \mu f_0(980))$ improves the estimate of [18] in several aspects. First, we demand compatibility with present data on light neutrino masses and mixings. Second, we do not use the mass insertion approximation, we take into account the full set of SUSY one-loop diagrams in the LFV vertex $\tau\mu H$ ($H = h^0, H^0$), and include the two contributions mediated by the h_0 and H_0 respectively. Consequently, we explore the full $5 \leq \tan\beta \leq 60$ interval. Besides, the hadronization of quark bilinears into the $f_0(980)$ meson is performed here quite differently than in [18], where a simplified quark-flavour scheme was used to express these bilinears in terms of phenomenological meson decay constants. We instead pay close attention to the chiral constraints, following the standard Chiral Perturbation Theory (χ PT) [41–43] and the Resonance Chiral Theory ($\text{R}\chi\text{T}$) [44–48] to incorporate resonances. Concretely, we follow the description of $f_0(980)$ in [47], where it is defined by a mixing between the octet and singlet components of the nonet of the scalar resonances which are included in $\text{R}\chi\text{T}$. Furthermore, we do not work in a generic Minimal Supersymmetric Standard Model (MSSM) but in constrained models with input parameters set at the high energies. Concretely we focus on two particular constrained SUSY scenarios of remarkable interest: the usual constrained MSSM (CMSSM) scenario [49], with universal soft SUSY masses at the gauge coupling unification scale, and the so-called Non-Universal Higgs Mass (NUHM) scenario [50], with all the scalar soft masses been universal except for the Higgs sector ones. In this later case the predicted Higgs masses, m_{h^0} and m_{H^0} , can be both light, $\sim 100 - 250$ GeV, indeed close to their present experimental lower bounds and, therefore, the corresponding Higgs mediated contribution to the previous LFV process can be relevant, even for large soft SUSY masses at ~ 1000 GeV. This is precisely the main interest of the channel $\tau \rightarrow \mu f_0(980)$, namely, the fact that the decay rates can be sizeable even at large $M_{\text{SUSY}} \sim \mathcal{O}(1 \text{ TeV})$, in clear contrast with other competitive tau flavour violating channels like $\tau \rightarrow \mu\gamma$, whose rates decrease as $1/M_{\text{SUSY}}^2$ and lay below the present experimental bound for such a heavy SUSY spectrum.

2 Framework for the $\tau \rightarrow \mu f_0(980)$ decay

For the present study of the $\tau \rightarrow \mu f_0(980)$ decay, we choose a SUSY-Seesaw framework where the spectrum of the MSSM is enlarged by three right-handed neutrinos, ν_{R_i} ($i = 1, 2, 3$), and

their SUSY partners, $\tilde{\nu}_{R_i}$ ($i = 1, 2, 3$). Here we assume a seesaw mechanism for neutrino mass generation and use, in particular, the parameterization proposed in [6] where the solution to the seesaw equation, relating the parameters of the six physical Majorana neutrinos, ν_i , and N_i ($i = 1, 2, 3$) to the neutrino Yukawa couplings, is written as

$$m_D = Y_\nu v_2 = i \sqrt{m_N^{\text{diag}}} R \sqrt{m_\nu^{\text{diag}}} U_{\text{PMNS}}^\dagger. \quad (1)$$

Here, the Dirac mass, m_D , the Yukawa neutrino coupling, Y_ν , and R are 3×3 matrices with full structure in flavour space. The orthogonal matrix R is defined by three complex angles θ_i ($i = 1, 2, 3$) [6]. $m_\nu^{\text{diag}} = \text{diag}(m_{\nu_1}, m_{\nu_2}, m_{\nu_3})$ denotes the three light neutrino masses, and $m_N^{\text{diag}} = \text{diag}(m_{N_1}, m_{N_2}, m_{N_3})$ the three heavy ones. The two Higgs vacuum expectation values are $v_{1(2)} = v \cos(\sin)\beta$, with $v = 174$ GeV. The Pontecorvo-Maki-Nakagawa-Sakata unitary matrix U_{PMNS} [51, 52] is given by the three (light) neutrino mixing angles θ_{12}, θ_{23} and θ_{13} , and three phases, δ, ϕ_1 and ϕ_2 . With this parameterization is easy to accommodate the neutrino data. It further allows for large Yukawa couplings $Y_\nu \sim \mathcal{O}(1)$ by choosing large entries in m_N^{diag} and/or θ_i .

For the numerical predictions in this work we will set:

$$\begin{aligned} m_{\nu_1}^2 &\simeq 0, & m_{\nu_2}^2 &= \Delta m_{\text{sol}}^2 = 8 \times 10^{-5} \text{ eV}^2, & m_{\nu_3}^2 &= \Delta m_{\text{atm}}^2 = 2.5 \times 10^{-3} \text{ eV}^2, \\ \theta_{12} &= 30^\circ, & \theta_{23} &= 45^\circ, & \theta_{13} &= 5^\circ, & \delta &= \phi_1 = \phi_2 = 0, \end{aligned} \quad (2)$$

which are compatible with present neutrino data [24], and consider the two possibilities for the heavy neutrinos: 1) Degenerate, with $m_{N_1} = m_{N_2} = m_{N_3} \equiv m_N$; and 2) Hierarchical, with $m_{N_1} \ll m_{N_2} \ll m_{N_3}$. This later case is well known to provide a plausible scenario for the Baryon Asymmetry of the Universe (BAU) via leptogenesis.

Regarding the SUSY parameters we will work within two different constrained MSSM-seesaw scenarios, the CMSSM with universal soft SUSY breaking parameters (including the extended sneutrino sector) and the NUHM model with non-universal Higgs soft masses. Thus, in addition to the previous neutrino parameters, m_{N_i} and θ_i , the input parameters of these two models are respectively,

$$\begin{aligned} \text{CMSSM} : & M_0, M_{1/2}, A_0, \tan \beta, \text{sign}(\mu), \\ \text{NUHM} : & M_0, M_{1/2}, A_0, \tan \beta, \text{sign}(\mu), M_{H_1}^2 = M_0^2 (1 + \delta_1), M_{H_2}^2 = M_0^2 (1 + \delta_2). \end{aligned} \quad (3)$$

where $M_0, M_{1/2}$ and A_0 are the universal soft SUSY breaking scalar masses, gaugino masses and trilinear couplings respectively at the gauge coupling unification scale, $M_X \simeq 2 \times 10^{16}$ GeV. The other parameters are, as usual, the ratio of the two Higgs vacuum expectation

values, $\tan \beta = v_2/v_1$, and the sign of the μ parameter, $\text{sign}(\mu)$. Notice, that the departure from universality in the soft Higgs masses of the NUHM is parameterized here in terms of the two dimensionless parameters δ_1 and δ_2 . Consequently, by taking $\delta_1 = \delta_2 = 0$ in the NUHM one recovers the CMSSM case. Finally, in order to evaluate the previous SUSY parameters and the physical masses at low energies (taken here as the Z gauge boson mass m_Z), we solve the full one-loop Renormalization Group Equations (RGEs) including the extended neutrino and sneutrino sectors. For this and the computation of the full spectra at the low energy we use here the public FORTRAN code SPheno [53]. In the numerical estimates we will set $M_0 = M_{1/2}$, $A_0 = 0$ and $\text{sign}(\mu) = +1$, for simplicity.

For the purpose of the present analysis the most relevant difference between the two previous constrained SUSY-seesaw scenarios is the spectrum of the Higgs sector. In particular, we want to explore the interesting case where the neutral Higgs bosons that mediate the $\tau \rightarrow \mu f_0(980)$ decay are light, while keeping the SUSY spectra heavy enough as to suppress the other competitive LFV tau decay channels like, for instance, $\tau \rightarrow \mu \gamma$. This is clearly possible within the NUHM-seesaw scenario, as illustrated in Fig. 1. We see in this figure that, by

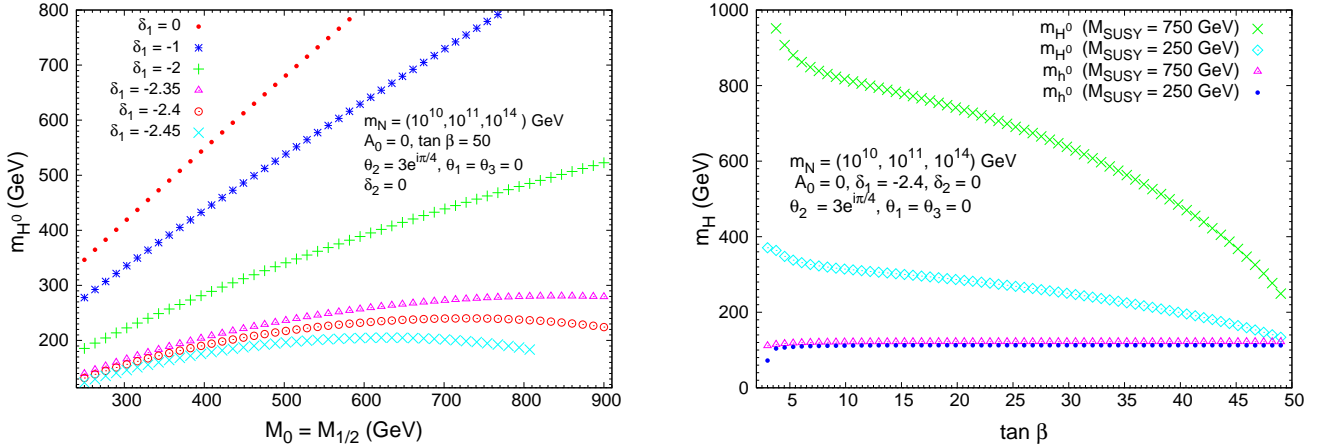


Figure 1: CP-even Higgs boson masses in the NUHM-Seesaw scenario: 1) m_{H^0} as a function of $M_{SUSY} = M_0 = M_{1/2}$ for several input $\delta_{1,2}$ (left panel). The predictions in the CMSSM-Seesaw scenario ($\delta_1 = \delta_2 = 0$) are included for comparison; 2) m_{H^0} and m_{h^0} as functions of $\tan \beta$ for $M_{SUSY} = 250$ GeV and 750 GeV (right panel).

properly adjusting the input δ_1 and δ_2 parameters, the heavy Higgs boson H^0 can get masses as low as 100-250 GeV even for a very heavy SUSY spectrum. For instance, for $\delta_1 = -2.4$, $\delta_2 = 0$, $\tan \beta = 50$, $M_{SUSY} = M_0 = M_{1/2} = 750$ GeV and the other input parameter values as specified in this figure, we get $m_{H^0} = 249$ GeV and $m_{h^0} = 122$ GeV, to be compared with

$m_{H^0} = 998$ GeV and $m_{h^0} = 122$ GeV of the CMSSM-Seesaw case. With choices for $\delta_2 \neq 0$ one gets even lower values of m_{H^0} . For the following numerical analysis and, for simplicity, we will set, however, $\delta_2 = 0$ and play just with δ_1 . It is worth also mentioning that the predictions for m_{A^0} (not shown in this figure) are practically indistinguishable from those of m_{H^0} .

Within the previous scenarios for the neutrino and SUSY sectors, it is well known that one can get large LFV decay rates if one chooses large entries in m_N^{diag} and/or complex θ_i , basically due to the large size of Y_ν in these models. This can be understood more easily in the Leading Logarithmic (LLog) approximation where, the tau-muon flavour violation, which is of our interest here, is qualitatively well described by the parameter,

$$\delta_{32} = -\frac{1}{8\pi^2} \frac{(3M_0^2 + A_0^2)}{M_{\text{SUSY}}^2} (Y_\nu^\dagger L Y_\nu)_{32}, \quad L_{kl} \equiv \log\left(\frac{M_X}{m_{N_k}}\right) \delta_{kl}, \quad k, l = 1, 2, 3, \quad (4)$$

where M_{SUSY} is an average SUSY mass. The size of $|\delta_{32}|$ can be indeed quite large. For instance, for mass values of the heavy neutrinos m_{N_3} (or m_N) in the range $10^{14} - 10^{15}$ GeV and θ_i ($i=1$ or/and 2) with large modulus in the range $3 - 5$ or/and large argument in the range $[\pm\pi/4, \pm\pi/2]$ one can get values of $|\delta_{32}|$ as large as 0.5-10. This is clearly illustrated in the contour plots of Fig. 2, where we have considered both scenarios with either degenerate or hierarchical heavy neutrinos and we have explored in the (m_{N_i}, θ_i) parameter space. In the hierarchical case the relevant mass is the heaviest one m_{N_3} and the predictions for $|\delta_{32}|$ do not vary appreciably with $m_{N_{1,2}}$. In addition, we have checked that $|\delta_{32}|$ is nearly constant with θ_3 . The contour plots for θ_1 (not shown) are very similar to those of θ_2 . We have also found that the largest values of $|\delta_{32}|$ are obtained for the degenerate case with both θ_1 and θ_2 being large. This is also clearly illustrated in the lower right panel of Fig. 2. For instance, we get $|\delta_{32}| \simeq 5$ for $m_N = 10^{14}$ GeV and $\theta_1 = \theta_2 = 3 \exp(i\pi/4)$. Notice also that values of $|\delta_{32}|$ larger than ~ 0.5 correspond in our parameterization of the Yukawa coupling matrices in (1) to values of $|Y_\nu|^2/(4\pi)$ that are above the threshold where the SPheno code sets the limit of perturbativity, which is at $|Y_\nu|^2/(4\pi) \sim 1.5$. It means that, in the following, we will be able to provide full predictions for the decay rates with the SPheno code only for those model parameters producing Y_ν values that are within the perturbativity region or, equivalently, leading to $|\delta_{32}| < 0.5$. The implications for the $\tau \rightarrow \mu f_0(980)$ decay of values $|\delta_{32}| \geq 0.5$ will be explored later, not with our full computation implemented by us in SPheno, but using an approximate formula that will also be presented here and that turns to work reasonably well.

Next, we specify our framework for the hadronization of the quark bilinears into the $f_0(980)$ meson. We use here the chiral Lagrangian of R χ T that is a suitable tool to realise

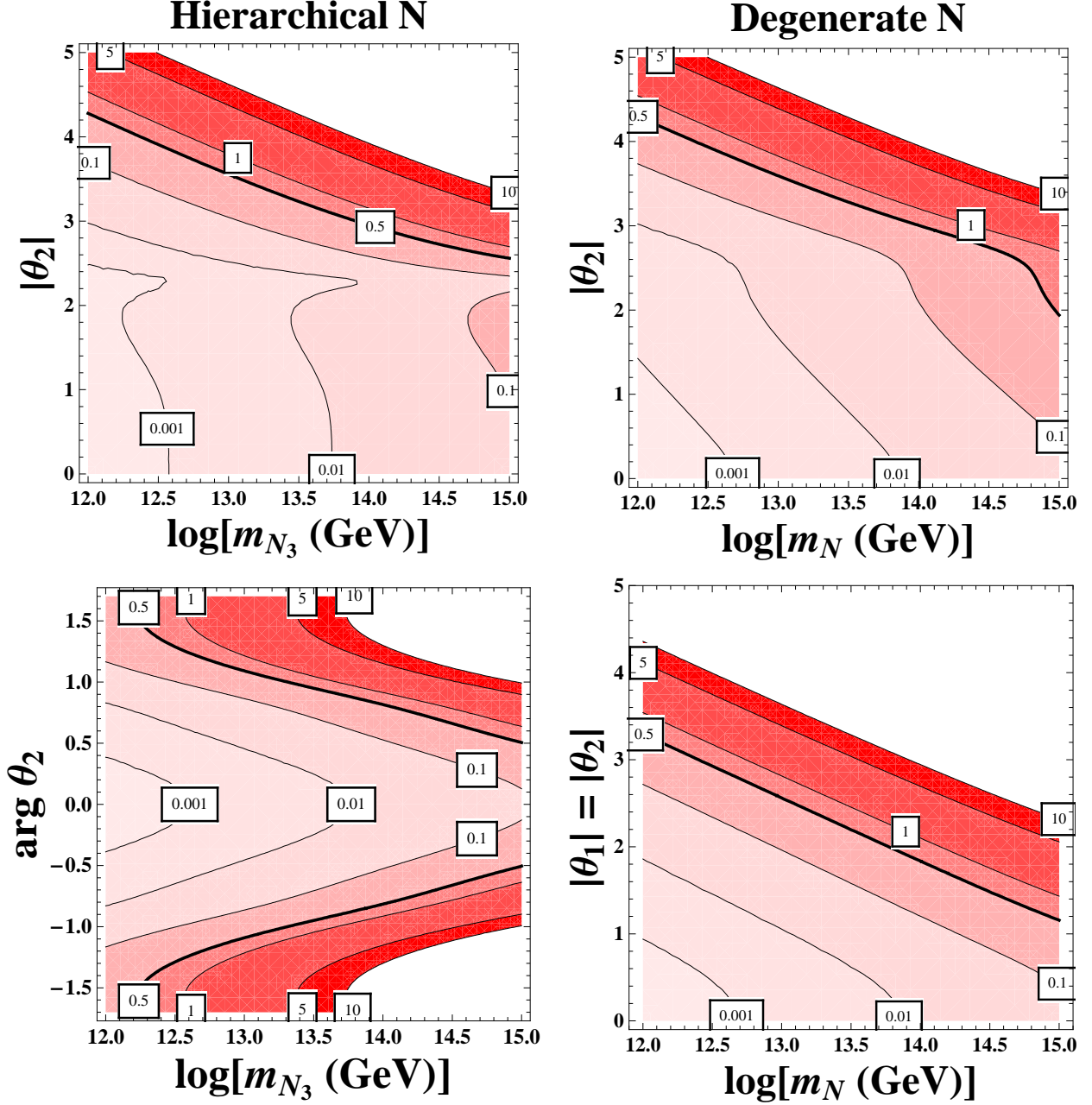


Figure 2: Contours of $|\delta_{32}|$ in the CMSSM-seesaw scenario: 1) For hierarchical heavy neutrinos. Upper left panel: in the $(|\theta_2|, m_{N_3})$ plane for $\arg \theta_2 = \pi/4$. Lower left panel: in the $(\arg \theta_2, m_{N_3})$ plane for $|\theta_2| = 3$. The other heavy neutrino parameters are set to $\theta_1 = \theta_3 = 0$, $m_{N_1} = 10^{10}$ GeV, $m_{N_2} = 10^{11}$ GeV; 2) For degenerate heavy neutrinos. Upper right panel: in the $(|\theta_2|, m_N)$ plane for $\arg \theta_2 = \pi/4$ and $\theta_1 = \theta_3 = 0$. Lower right panel: in the $(|\theta_1| = |\theta_2|, m_N)$ plane for $\arg \theta_1 = \arg \theta_2 = \pi/4$, and $\theta_3 = 0$. In all plots we have set: $M_{\text{SUSY}} = M_0 = M_{1/2}$, $A_0 = 0$, $\tan \beta = 50$, and the θ_i are expressed in radians.

the $1/N_C$ expansion of $SU(N_C)$ QCD and includes both the Goldstone bosons $\Phi(\pi, K$ and $\eta)$ and the resonances as active degrees of freedom, and their interactions. For the present work, it is sufficient to consider the lightest nonet of scalar resonances $R(0^+)$ in $R\chi T$,

$$\mathcal{L}_{R\chi T} = \mathcal{L}_\chi^{(2)} + \mathcal{L}_{\text{kin}}^R + \mathcal{L}_{(2)}^R, \quad (5)$$

where,

$$\begin{aligned} \mathcal{L}_\chi^{(2)} &= \frac{F^2}{4} \langle u_\mu u^\mu + \chi_+ \rangle, \quad F \simeq F_\pi \simeq 92.4 \text{ MeV}, \\ \mathcal{L}_{\text{kin}}^R &= \frac{1}{2} \langle \nabla^\mu R \nabla_\mu R - M_R^2 R^2 \rangle, \\ \mathcal{L}_{(2)}^R &= c_d \langle R u_\mu u^\mu \rangle + c_m \langle R \chi_+ \rangle, \end{aligned} \quad (6)$$

and $\langle \dots \rangle$ is short for a trace in the flavour space. The other quantities in (6) are:

$$\begin{aligned} u_\mu &= i[u^\dagger(\partial_\mu - ir_\mu)u - u(\partial_\mu - i\ell_\mu)u^\dagger], & u &= \exp[i\Phi/(\sqrt{2}F)], \\ \chi_+ &= u^\dagger \chi u^\dagger + u \chi^\dagger u, & \chi &= 2B_0(s + ip), \\ \nabla_\mu R &= \partial_\mu R + [\Gamma_\mu, R], & \Gamma_\mu &= \frac{1}{2} [u^\dagger(\partial_\mu - ir_\mu)u + u(\partial_\mu - i\ell_\mu)u^\dagger], \end{aligned} \quad (7)$$

being Φ the nonet of Goldstone bosons and ℓ_μ, r_μ, s and p the nonets of left, right, scalar and pseudoscalar external fields, respectively. Short-distance dynamics [46] constraints the couplings of $R\chi T$ by imposing the QCD ruled behaviour of Green functions and associated form factors. For the couplings in $\mathcal{L}_{(2)}^R$ one gets¹ :

$$2c_m = 2c_d = F. \quad (8)$$

Finally the chiral tensor χ gives masses to the Goldstone bosons through the external scalar field. In the isospin limit one has :

$$\begin{aligned} 2B_0 m_u &= 2B_0 m_d = m_\pi^2, \\ 2B_0 m_s &= 2m_K^2 - m_\pi^2. \end{aligned} \quad (9)$$

The QCD spectrum of scalar resonance states is far from being settled and constitutes, at present, a highly debated issue. It is not our goal in this article to enter in the details of the discussion and, therefore, we will attach to the scheme put forward in [47] for the description

¹Short-distance constraints on the $R\chi T$ couplings depend on the operators included. The result in (8) is obtained when only linear operators in the resonances are considered [44]. A weaker constraint, though compatible with that result, arises if non-linear couplings in the resonances are included [48].

of the isosinglet $f_0(980)$ state. The later is defined as a rotation of the octet R_8 and the singlet R_0 components of the $R(0^+)$ nonet,

$$\begin{pmatrix} R_8 \\ R_0 \end{pmatrix} = \begin{pmatrix} \cos \theta_S & \sin \theta_S \\ -\sin \theta_S & \cos \theta_S \end{pmatrix} \begin{pmatrix} f_0(1500) \\ f_0(980) \end{pmatrix}. \quad (10)$$

The value of the θ_S mixing angle is uncertain. In the analysis carried out in [47] considering nonet breaking (i.e. subleading effects in the large- N_C expansion) a possible dual scenario is favoured :

- A) The candidates for the nonet are: $f_0(980)$, $K_0^*(1430)$, $a_0(1450)$ and $f_0(1500)$. In this framework the $a_0(980)$ is dynamically generated (through loops). The mixing angle, around $\theta_S \simeq 30^\circ$, provides a dominant non-strange component for the lightest $I = 0$ state and, consequently, justifies their dominant decay into two pions.
- B) The nonet would be composed by: $f_0(980)$, $a_0(980)$, $K_0^*(1430)$ and $f_0(1500)$. Hence $a_0(980)$ is a pre-existing state in the $N_C \rightarrow \infty$ limit. The mixing angle in this case is around $\theta_S \simeq 7^\circ$, that gives a noticeable strange component.

Given the uncertainty provided by the large corrections due to $1/N_C$ subleading effects we will consider the two previous scenarios for the $f_0(980)$ as plausible and will present estimates of the $\tau \rightarrow \mu f_0(980)$ decay rates for the two mixing angles, $\theta_S \simeq 7^\circ$ and $\theta_S \simeq 30^\circ$. The dispersion between these two results can be considered as part of the theoretical error in our estimates.

Finally, the hadronization of the relevant scalar quark bilinears into the $f_0(980)$ is implemented by replacing the following expressions in the results for the decay rates at the quark level,

$$\begin{aligned} \bar{u}u &= - \left[\frac{1}{2}S_3 + \frac{1}{2\sqrt{3}}S_8 + \frac{1}{\sqrt{6}}S_0 \right], \\ \bar{d}d &= - \left[-\frac{1}{2}S_3 + \frac{1}{2\sqrt{3}}S_8 + \frac{1}{\sqrt{6}}S_0 \right], \\ \bar{s}s &= - \left[-\frac{1}{\sqrt{3}}S_8 + \frac{1}{\sqrt{6}}S_0 \right], \end{aligned} \quad (11)$$

with

$$S_i = \frac{8}{\sqrt{2}} B_0 c_m R_i, \quad i = 0, 3, 8, \quad (12)$$

and, according to (8), $c_m = F/2$. As R_3 does not contain information on $f_0(980)$ (in the isospin limit) we will discard the S_3 contribution.

Before proceeding a word of caution is necessary when dealing with processes with resonances as initial or final states. A resonance is not an asymptotic state as it decays strongly. Hence from a quantum field theory point of view R χ T only describes the creation, propagation and destruction of resonances and the later should not appear as “in” or “out” states. For instance, in our case the physical process should be $\tau \rightarrow \mu\pi\pi$ mediated by a $f_0(980)$ state, and not $\tau \rightarrow \mu f_0(980)$. Then it would proceed to study the scalar state as we did with the vector ones in Ref. [21]. However the description of scalars, as has been pointed out, is far from clear and therefore considering the $f_0(980)$ as an asymptotic state should not increase effectively the already rather large uncertainty.

3 Results for BR($\tau \rightarrow \mu f_0(980)$)

Analytical results

The semileptonic $\tau \rightarrow \mu f_0(980)$ decay can be mediated by h^0 and H^0 Higgs bosons, as shown in Fig. 3. In this figure the LFV vertex is represented by a black circle and the hadronic vertex by a grey box. The total amplitude for this decay, $T_H = T_{h^0} + T_{H^0}$, is first evaluated at the quark level, that is for $\tau \rightarrow \mu\bar{q}q$, and then at the hadron level by substituting the quark bilinears by the corresponding scalar currents containing the $f_0(980)$ meson as evaluated from $\mathcal{L}_{R\chi T}$ in (5). The amplitude at the quark level can be computed in terms of the corresponding $\tau\mu H_p$ one-loop vertex functions, $H_{L,R}^{(p)}$, with $H_p = h^0, H^0$, resulting from the evaluation of the diagrams in Fig. 4 with sleptons, \tilde{l}_X , sneutrinos, $\tilde{\nu}_X$, charginos, $\tilde{\chi}_A^\pm$, and neutralinos, $\tilde{\chi}_A^0$, in the loops. The resulting amplitude at the quark level is given by:

$$T_H(\tau \rightarrow \mu\bar{q}q) = \sum_{h^0, H^0} \frac{1}{m_{H_p}^2} \left\{ H_L^{(p)} S_{L,q}^{(p)} [\bar{\mu} P_L \tau] [\bar{q} P_L q] + H_R^{(p)} S_{R,q}^{(p)} [\bar{\mu} P_R \tau] [\bar{q} P_R q] \right. \\ \left. + H_L^{(p)} S_{R,q}^{(p)} [\bar{\mu} P_L \tau] [\bar{q} P_R q] + H_R^{(p)} S_{L,q}^{(p)} [\bar{\mu} P_R \tau] [\bar{q} P_L q] \right\} . \quad (13)$$

where $P_{L,R} = (1 \mp \gamma_5)/2$, and

$$S_{L,q}^{(p)} = \frac{g}{2m_W} \left(\frac{-\sigma_2^{(p)*}}{\sin \beta} \right) m_q , \quad q = u ; \\ S_{L,q}^{(p)} = \frac{g}{2m_W} \left(\frac{\sigma_1^{(p)*}}{\cos \beta} \right) m_q , \quad q = d, s ; \\ S_{R,q}^{(p)} = S_{L,q}^{(p)*} \quad (14)$$

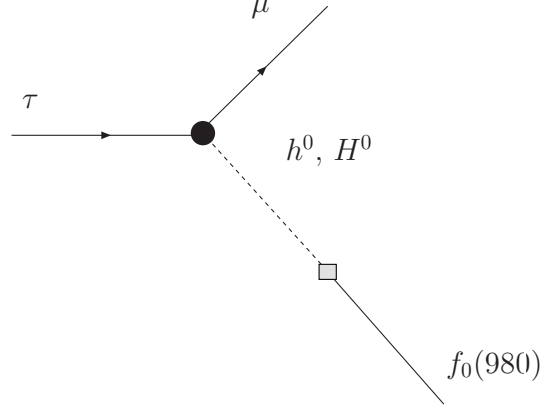


Figure 3: Higgs-mediated contributions to the LFV semileptonic $\tau \rightarrow \mu f_0(980)$ decay

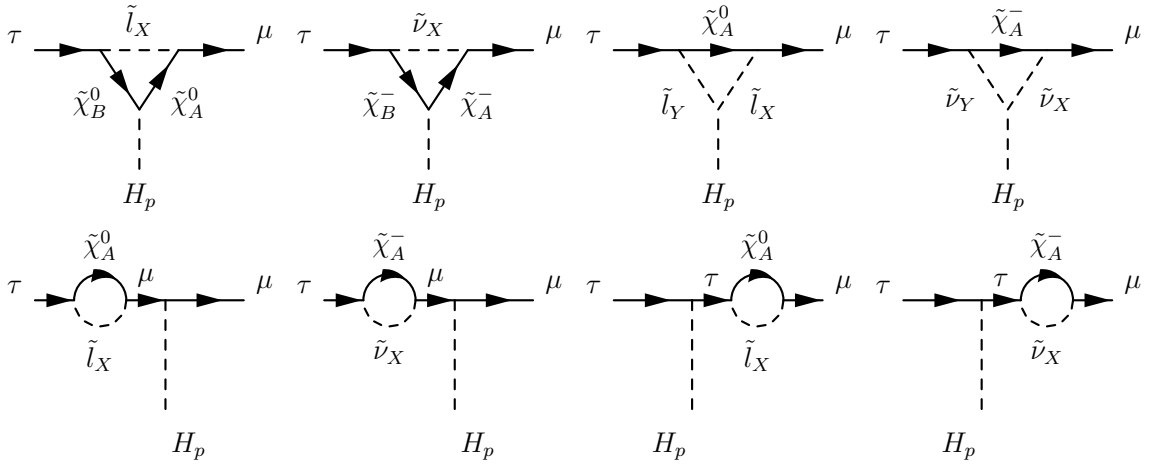


Figure 4: Relevant SUSY one-loop diagrams for the Higgs-mediated contributions to the $\tau \rightarrow \mu f_0(980)$ decay. Here $H_p = h^0, H^0$.

with

$$\sigma_1^{(p)} = \begin{pmatrix} \sin \alpha \\ -\cos \alpha \\ i \sin \beta \end{pmatrix}, \quad \sigma_2^{(p)} = \begin{pmatrix} \cos \alpha \\ \sin \alpha \\ -i \cos \beta \end{pmatrix}. \quad (15)$$

Here m_W is the W gauge boson mass and g the $SU(2)$ gauge coupling. The three entries in $\sigma_{1,2}^{(p)}$ are, in order from top to bottom, for $H_p = h^0, H^0, A^0$, respectively.

The results of the LFV vertex functions are taken from [14], and are not written here explicitly for shortness. Just to mention that it is a full one-loop computation, including all the contributions with charginos in the loops, $H_{L(R),c}^{(p)}$, and those with neutralinos, $H_{L(R),n}^{(p)}$.

Besides, all these contributions are written in terms of the physical particle masses. As we have mentioned before, these physical masses are computed here in the SUSY-seesaw scenario by solving the one-loop RGEs with SPheno and for a given set of universal (in the CMSSM) or non-universal conditions (for the NUHM) at the unification scale. Since the three right-handed neutrinos and their SUSY partners are included in the RGEs, they will affect as well in the predicted physical masses at the low energies.

To get the amplitude for the process $\tau \rightarrow \mu f_0(980)$ we substitute the quark bilinears of (11) in (13) and use (10) and (12). Notice that it is just the scalar part in $[\bar{q}P_{L,R}q]$, and not the pseudoscalar, the one that contributes in the present case. We obtain:

$$T_H(\tau \rightarrow \mu f_0(980)) = \sum_{p=h^0, H^0} c_p \bar{\mu} \tau, \quad (16)$$

where

$$c_p = \frac{g}{2m_W} \frac{1}{2m_{H_p}^2} \left(J_L^{(p)} + J_R^{(p)} \right) \left(H_R^{(p)} + H_L^{(p)} \right), \quad (17)$$

and

$$\begin{aligned} J_L^{(p)} &= \frac{c_m}{\sqrt{3}} \left\{ \frac{\sigma_2^{(p)*}}{\sin \beta} \left[\frac{1}{\sqrt{2}} \sin \theta_S + \cos \theta_S \right] m_\pi^2 \right. \\ &\quad \left. - \frac{\sigma_1^{(p)*}}{\cos \beta} \left[\frac{3}{\sqrt{2}} \sin \theta_S m_\pi^2 + \left(\cos \theta_S - \sqrt{2} \sin \theta_S \right) 2 m_K^2 \right] \right\}, \\ J_R^{(p)} &= J_L^{(p)*}. \end{aligned} \quad (18)$$

Notice that due to the mass relations in (9), the couplings of the Higgs bosons, h^0 and H^0 , to the quarks ($q = u, d, s$), $S_{L,q}^{(p)}$ and $S_{L,q}^{(p)}$ in (14), being proportional to the quark masses, lead to Higgs- f_0 couplings that are proportional to m_P^2 ($P = \pi, K$). This is seen clearly in the predicted functions $J_{L,R}^{(p)}$ of (18). In consequence, the dominant contributions to $\text{BR}(\tau \rightarrow \mu f_0(980))$ will come clearly from the terms in the amplitude that are proportional to m_K^2 .

Finally, the result of the branching ratio for the $\tau \rightarrow \mu f_0(980)$ decay is given by,

$$\text{BR}(\tau \rightarrow \mu f_0(980)) = \frac{1}{4\pi} \frac{\lambda^{1/2}(m_\tau^2, m_\mu^2, m_{f_0}^2)}{m_\tau^2 \Gamma_\tau} \frac{1}{2} \sum_{i,f} |T_H|^2, \quad (19)$$

where

$$\frac{1}{2} \sum_{i,f} |T_H|^2 = \frac{(m_\mu + m_\tau)^2 - m_{f_0}^2}{4 m_\tau} |c_{h^0} + c_{H^0}|^2, \quad (20)$$

being Γ_τ is the total τ width and $\lambda(x, y, z) = (x + y - z)^2 - 4xy$.

Approximate formula

Next we derive a simple formula which approximates reasonably well our full one-loop prediction in (19) and (20). For this, we work within the approximation of large $\tan\beta$ that is appropriate for LFV tau decays, whose rates grow quite fast with this parameter. This is especially relevant for channels where the LFV rates are dominated by the Higgs mediated diagrams, as it is the present case, and where the growth with $\tan\beta$ is extremely pronounced.

The other approximation which is used frequently in the literature, due to its simplicity, is the use of the mass insertion (MI) method, where the tau-muon LFV is encoded in the dimensionless parameters δ_{32}^{XY} ($XY = LL, RR, LR$). In the SUSY models the dominant one is δ_{32}^{LL} and its expression in the LLog approximation, $(\delta_{32}^{LL})_{\text{LLog}} \equiv \delta_{32}$, is that given in (4).

It is known [14] [16] that at large $\tan\beta$ the vertex function H_L dominates H_R by about a factor m_τ/m_μ . In addition $H_L^{H^0}$ is by far larger than $H_L^{h^0}$ in this limit, and one can safely neglect the later one. More specifically, by using the MI approximation, its chargino and neutralino contributions in the large $\tan\beta$ and heavy M_{SUSY} limits give, correspondingly, the following expressions :

$$\begin{aligned} H_{L,c}^{(H^0)} &= \frac{g^3}{16\pi^2} \frac{m_\tau}{12m_W} \delta_{32} \tan^2 \beta, \\ H_{L,n}^{(H^0)} &= \frac{g^3}{16\pi^2} \frac{m_\tau}{24m_W} (1 - 3 \tan^2 \theta_W) \delta_{32} \tan^2 \beta. \end{aligned} \quad (21)$$

One can further verify that H_c dominates H_n by about a factor 20, so that we will simplify $H_L \simeq H_{L,c}$.

On the other hand, we also consider the large $\tan\beta$ limit of the functions that define the H^0 couplings to $f_0(980)$, J_L and J_R in (18). We obtain :

$$J_L^{(H^0)} = J_R^{(H^0)} = \frac{F}{2\sqrt{3}} \tan\beta \left[\frac{3}{\sqrt{2}} \sin\theta_S m_\pi^2 + (\cos\theta_S - \sqrt{2} \sin\theta_S) 2m_K^2 \right]. \quad (22)$$

By using the above sequence of approximations and by neglecting the muon mass, we finally get the following simple result:

$$\begin{aligned} \text{BR}(\tau \rightarrow \mu f_0(980))_{\text{approx}} &= \frac{1}{16\pi m_\tau^3} (m_\tau^2 - m_{f_0}^2)^2 \left| \frac{g}{2m_W} \frac{1}{m_{H^0}^2} J_L^{(H^0)} H_{L,c}^{(H^0)} \right|^2 \frac{1}{\Gamma_\tau} \\ &= \left(\frac{7.3 \times 10^{-8} (\theta_S = 7^\circ)}{4.2 \times 10^{-9} (\theta_S = 30^\circ)} \right) |\delta_{32}|^2 \left(\frac{100}{m_{H^0}(\text{GeV})} \right)^4 \left(\frac{\tan\beta}{60} \right)^6. \end{aligned} \quad (23)$$

In the last line we see explicitly the fast growth with $\tan \beta$, as $(\tan \beta)^6$, the expected dependence with the relevant Higgs mass, as $(m_{H^0})^{-4}$, and also with the LFV parameter, as $|\delta_{32}|^2$. The two numerical factors correspond to the two assumed values for the mixing angle that defines the $f_0(980)$ state, $\theta_S = 7^\circ$ and $\theta_S = 30^\circ$. These two numbers differ by a factor 17, meaning that the predicted rates will carry a theoretical uncertainty of about this number, due to the uncertainty in the definition of the $f_0(980)$ state.

Numerical results

In the following we present the numerical predictions for $\text{BR}(\tau \rightarrow \mu f_0(980))$. We first show the results from the full computation in (19) and (20) and then compare with the approximate results in (23) and also with the rates of other LFV tau decay channels.

In Fig. 5 it is shown the $\text{BR}(\tau \rightarrow \mu f_0(980))$ versus the heavy neutrino masses, in both scenarios with hierarchical and degenerate heavy neutrinos. In the hierarchical case we display just the dependence with the relevant mass, m_{N_3} . As expected, from the previously manifested behaviour of $|\delta_{32}|$ with m_{N_3} (or with m_N , in the degenerate case) in Fig. 2, we find a fast growing of $\text{BR}(\tau \rightarrow \mu f_0(980))$ with this mass. Although not explicitly shown here, we have also checked in the hierarchical case, the near independence on the other masses, m_{N_1} and m_{N_2} . From this figure it is also evident that by choosing properly the δ_1 and δ_2 parameters of the NUHM scenario, such that the relevant Higgs boson mass m_{H^0} gets lower than for $\delta_1 = \delta_2 = 0$, the branching ratios get larger than in the CMSSM scenario. Finally, by comparing the rates of the two neutrino scenarios, and for the same input model parameter values, including the same m_N and m_{N_3} , we find rates in the degenerate case that are generally larger than in the hierarchical case. For instance, for the choice of input parameters in Fig. 5 we find larger rates by a factor of about 3. In the following we will focus more on the hierarchical case since it has the appealing feature of providing successful baryogenesis, via leptogenesis, for some regions of the heavy neutrino parameter space.

We present the predictions of the $\text{BR}(\tau \rightarrow \mu f_0(980))$ versus the soft SUSY masses M_0 and $M_{1/2}$ in Fig. 6. Here we take again $M_0 = M_{1/2} \equiv M_{\text{SUSY}}$ and compare the results in both scenarios, the NUHM with $\delta_1 = -2.4$ and $\delta_2 = 0$, where the predicted Higgs boson masses for large $\tan \beta \sim 50$ lay within the interval 100-250 GeV, and the CMSSM. The most evident feature in this plot is the different behaviour of the $\text{BR}(\tau \rightarrow \mu f_0(980))$ with M_{SUSY} in these two scenarios. Whereas in the CMSSM the rates are found to decrease with increasing M_{SUSY} , as expected, it clearly does not happen in the NUHM. In fact, the rates are practically constant for $M_{\text{SUSY}} > 400$ GeV. The reason for this behaviour is that the SUSY particles do not decouple at large M_{SUSY} in this decay. The non-decoupling behaviour can be checked analytically in that the LFV vertex, described by the dominant form factor

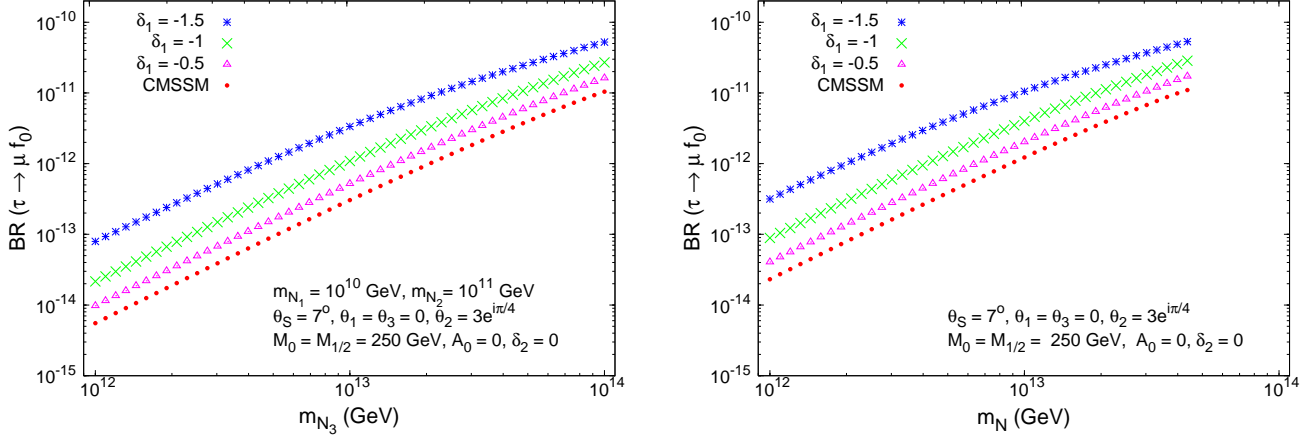


Figure 5: $\text{BR}(\tau \rightarrow \mu f_0(980))$ in the NUHM-seesaw, for several δ_1 values, and in the CMSSM-seesaw versus the relevant heavy neutrino mass, 1) for hierarchical heavy neutrinos (left panel), and 2) degenerate heavy neutrinos (right panel).

H_L , tends to a constant value at asymptotically large M_{SUSY} , as indicated in (21). Since, on the other hand, m_{H^0} is kept at the low region even for large M_{SUSY} , then a constant H_L with M_{SUSY} implies approximately constant $\text{BR}(\tau \rightarrow \mu f_0(980))$ as well.

Another interesting feature of the predicted rates in the NUHM scenario, that is manifested in Fig. 6 as well, is the clear dominance by many orders of magnitude of the H^0 contribution over the h^0 one in the whole M_{SUSY} considered interval. This is due to the fact that at large $\tan\beta$ the H^0 contribution is enhanced by a $\tan^6\beta$ factor, whereas the h^0 one is suppressed in this limit. In fact, we also see in this plot that the total rates are nearly indistinguishable from the H^0 contributions. Thus, to neglect the h^0 contribution is an extremely good approximation.

Concerning the Higgs sector parameters, the $\text{BR}(\tau \rightarrow \mu f_0(980))$ is mainly sensitive to $\tan\beta$ and m_{H^0} since, as said before, the H^0 -mediated LFV semileptonic decays grow very fast with both $\tan\beta$ and $1/m_{H^0}$. In fact, in the approximation given in (23), as already said, $\text{BR}(\tau \rightarrow \mu f_0(980))$ goes as $(\tan\beta)^6$ and $(1/m_{H^0})^4$, respectively.

The predictions of $\text{BR}(\tau \rightarrow \mu f_0(980))$ as a function of $\tan\beta$ are shown in the right panel of Fig.6. We show again separately the h^0 and H^0 contributions and the total rates which are clearly dominated by the H^0 in the full studied interval of $\tan\beta$. Besides, it also displays the fast growing of the total rates with $\tan\beta$, reaching values at the $\sim 10^{-9}$ level for $\tan\beta \sim 50$ which are close but still below the present experimental bound. We also see

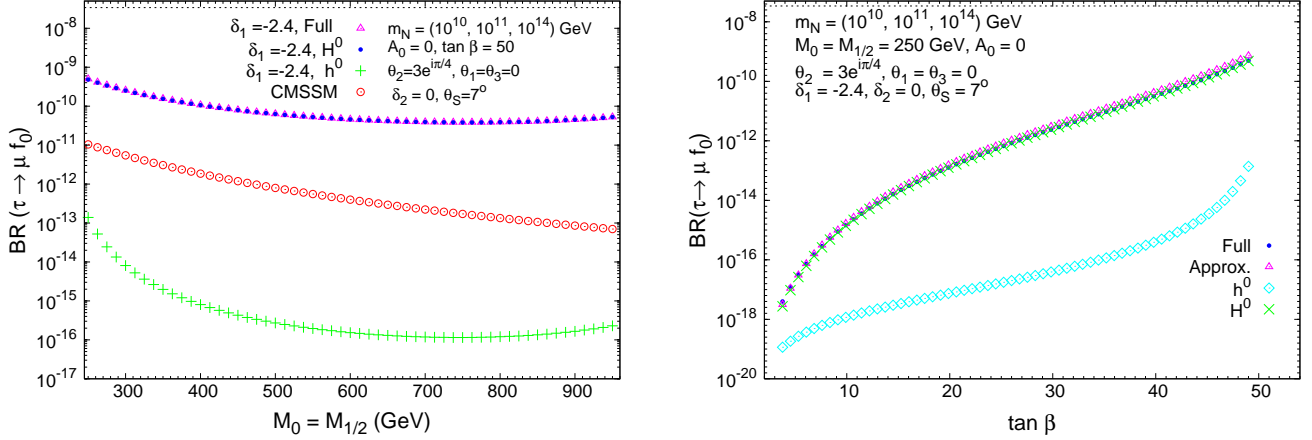


Figure 6: $\text{BR}(\tau \rightarrow \mu f_0(980))$ in the NUHM-Seesaw scenario: 1) As a function of $M_0 = M_{1/2} = M_{\text{SUSY}}$ (left panel). We show separately the H^0 and h^0 contributions as well as the total. The predictions for the total rates within the CMSSM-Seesaw scenario are also included for comparison; 2) As a function of $\tan \beta$ (right panel). Again, the dominant H^0 , the subdominant h^0 and the total rates are displayed. We also include here the approximate predictions given by (23) for comparison with the full rates.

that the particular shape of the curve for the total rates is a consequence as well of the m_{H^0} dependence with $\tan \beta$ in these SUSY scenarios, as illustrated in Fig. 1.

The comparison between our predictions for the full result in (19) and (20) and the approximate results in (23), which include just the H^0 boson contribution, can be seen as well in Fig. 6. The agreement between the full and the approximate results is quite remarkable, for all the studied values in the $5 \lesssim \tan \beta \lesssim 50$ range. Therefore, we conclude that our simple formula (23) provides a very good approximation to $\text{BR}(\tau \rightarrow \mu f_0(980))$ for all $\tan \beta$.

It is interesting to compare $\tau \rightarrow \mu f_0(980)$ to other Higgs-mediated LFV tau decay channels like $\tau \rightarrow \mu \eta$ and $\tau \rightarrow 3\mu$. First, notice that our previous result of the H^0 dominance in the $\tau \rightarrow \mu f_0(980)$ channel over the full $\tan \beta$ interval, is not true for the correlated channel $\tau \rightarrow \mu \eta$, nor the leptonic $\tau \rightarrow 3\mu$ decay. The semileptonic LFV $\tau \rightarrow \mu \eta$ decay can be mediated by a CP-odd A^0 Higgs boson and a Z boson, but the contribution from A^0 dominates the full rates only in the large $\tan \beta \gtrsim 20$ region [21, 23]. The $\tau \rightarrow 3\mu$ channel can be mediated (apart from the box diagrams, which are negligible) by a photon, a Z boson and the three neutral Higgs bosons, h^0 , H^0 and A^0 [16]. The photon dominates largely this decay, except at the extreme high values of $\tan \beta \geq 60$ and $M_{\text{SUSY}} \geq 1$ TeV, where the two type of contributions from the photon and the Higgs bosons, H^0 and A^0 compete. These

features can be seen clearly by comparing the corresponding approximate formulas, valid at large $\tan\beta$, for their respective Higgs boson contributions. That is, one should compare our result in (23) to the previous results of $\text{BR}(\tau \rightarrow \mu\eta)$ [13, 21] and $\text{BR}(\tau \rightarrow 3\mu)$ [8, 10, 12, 16] for the same input parameters. These are [21],

$$\begin{aligned}\text{BR}(\tau \rightarrow \mu\eta)_{H_{\text{approx}}} &= \frac{1}{8\pi m_\tau^3} (m_\tau^2 - m_\eta^2)^2 \left| \frac{g}{2m_W} \frac{F}{m_{A^0}^2} B_L^{(A^0)}(\eta) H_{L,c}^{(A^0)} \right|^2 \frac{1}{\Gamma_\tau} \\ &= 1.2 \times 10^{-7} (\theta = -18^\circ) |\delta_{32}|^2 \left(\frac{100}{m_{A^0}(\text{GeV})} \right)^4 \left(\frac{\tan\beta}{60} \right)^6, \quad (24)\end{aligned}$$

where,

$$B_L^{(A^0)}(\eta) = -i \frac{1}{4\sqrt{3}} \tan\beta \left[(3m_\pi^2 - 4m_K^2) \cos\theta - 2\sqrt{2}m_K^2 \sin\theta \right], \quad H_{L,c}^{(A^0)} = iH_{L,c}^{(H^0)}, \quad (25)$$

and:

$$\text{BR}(\tau \rightarrow 3\mu)_{H_{\text{approx}}} = \frac{G_F^2 m_\tau^7 m_\mu^2}{2048\pi^3 \Gamma_\tau} \left(\frac{1}{m_{H^0}^4} + \frac{1}{m_{A^0}^4} + \frac{2}{3m_{H^0}^2 m_{A^0}^2} \right) \left| \frac{g^2 \delta_{32}}{96\pi^2} \right|^2 (\tan\beta)^6 \quad (26)$$

$$= 1.2 \times 10^{-7} |\delta_{32}|^2 \left(\frac{100}{m_{A^0}(\text{GeV})} \right)^4 \left(\frac{\tan\beta}{60} \right)^6. \quad (27)$$

From this comparison, we conclude that, for the same choice of the model parameters, and for $\theta_S = 7^\circ$, the three rates $\text{BR}(\tau \rightarrow \mu f_0(980))$, $\text{BR}(\tau \rightarrow \mu\eta)$ and $\text{BR}(\tau \rightarrow 3\mu)$ are very similar if $\tan\beta \gtrsim 60$ and $M_{\text{SUSY}} \gtrsim 1$ TeV. Concretely, we predict $\text{BR}(\tau \rightarrow \mu f_0(980)):\text{BR}(\tau \rightarrow 3\mu):\text{BR}(\tau \rightarrow \mu\eta) \sim 0.6 : 1 : 1$, and they are all at the $\sim \mathcal{O}(10^{-7})$ level for $|\delta_{32}| \sim 1$, $m_H \sim 100$ GeV and $\tan\beta \sim 60$. Therefore, the three are closely competitive channels. It should also be mentioned that our estimate of $\text{BR}(\tau \rightarrow \mu f_0(980))$ for $\theta_S \simeq 7^\circ$ and for the same input parameters, m_H , $\tan\beta$ and $|\delta_{32}|$, is about one order of magnitude smaller than the prediction in [18]. They also predict a different ratio among the three LFV channels of $\sim 1.3 : 0.5 : 1$. We believe that the main differences come from our different approaches for hadronization which produce, as we have already said, a dispersion in the results of about this factor.

Finally, we summarize the sensitivity to the Higgs sector in the NUHM-seesaw scenario in Fig.7. In this plot we are using the approximate formula in (23) and we are setting $\theta_2 = 3e^{i\frac{\pi}{4}}$ and $\delta_1 = -2.4$, $\delta_2 = 0$. The soft masses are varied in the range $200 \text{ GeV} \leq M_0 = M_{1/2} \equiv M_{\text{SUSY}} \leq 750 \text{ GeV}$. The explored m_{H^0} values in this plot correspond precisely to the output Higgs masses for this later M_{SUSY} interval. The main conclusion from this plot is that for large $m_{N_3} \sim 5 \times 10^{14} - 10^{15}$ GeV and large $\tan\beta \sim 50 - 60$ the predicted rates are

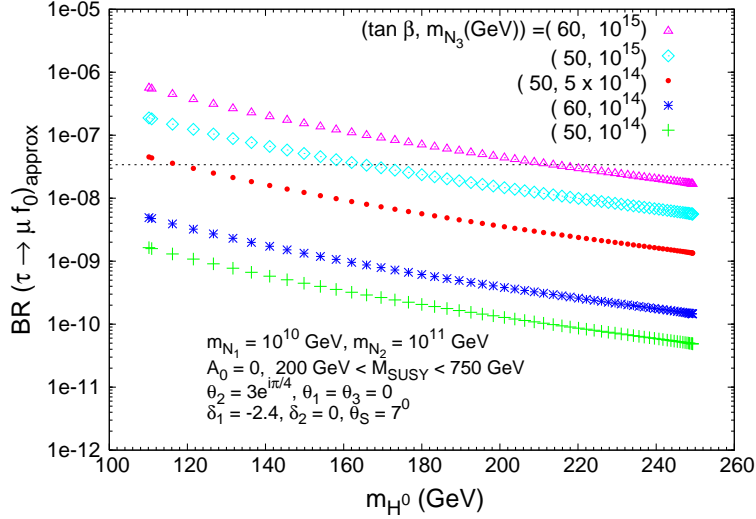


Figure 7: Sensitivity to the Higgs Sector in $\tau \rightarrow \mu f_0(980)$ within the NUHM-seesaw scenario. The predicted rates are within the approximation of (23) and are displayed as a function of m_{H^0} , for various choices of large m_{N_3} and $\tan \beta$.

already at the present experimental reach and, therefore, there is indeed Higgs sensitivity in this channel. In this concern, we find interesting to further explore if with the present experimental bound of $\text{BR}(\tau \rightarrow \mu f_0(980)) \times \text{BR}(f_0(980) \rightarrow \pi^+ \pi^-) < 3.4 \times 10^{-8}$ one may already exclude some region of the model parameter space. Our conclusion is that indeed it is possible to exclude the regions in the $(m_{H^0}, \tan \beta)$ plane as summarized in Fig. 8. In this plot we assume, for simplicity, $\text{BR}(f_0(980) \rightarrow \pi^+ \pi^-) \sim 1$ and choose the specific input values, $|\delta_{32}| = 0.1, 0.5, 1, 5, 10$. For each fixed $|\delta_{32}|$ the excluded region is the area above the corresponding contour line. For completeness, we have also included in this plot the present experimental lower bound for the SM Higgs mass at 114.4 GeV. Some words of caution should be said, anyway, about the conclusions from this plot since there are large uncertainties involved in the theoretical estimate of $\text{BR}(\tau \rightarrow \mu f_0(980))$. There are two main ones: 1) the uncertainty in the definition of $f_0(980)$ that, as evaluated in (23), can produce a dispersion of more than one order of magnitude in the predicted rates, and 2) the use of the approximate formula for values of $|\delta_{32}| > 0.5$ which are out of the region that is allowed by a perturbative approach. The use of the MI approximation for such large values of $|\delta_{32}|$ is also questionable.

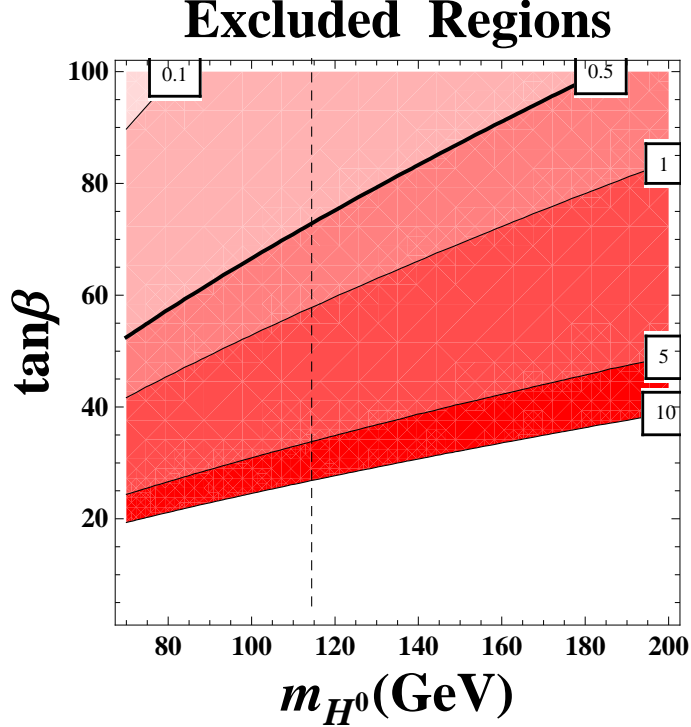


Figure 8: The excluded regions in the $(m_{H^0}, \tan \beta)$ plane are the areas above the contour lines corresponding to fixed $|\delta_{32}| = 0.1, 0.5, 1, 5, 10$.

4 Conclusions

In this work we have studied in full detail the LFV semileptonic tau decay channel $\tau \rightarrow \mu f_0(980)$ within the context of two constrained SUSY-seesaw models, the CMSSM-seesaw and the NUHM-seesaw which have very different Higgs sector spectra. Concretely, we have selected NUHM-seesaw scenarios with a light Higgs sector, h^0 , H^0 and A^0 , in the 100-250 GeV range, and considered several possibilities for the SUSY sector, varying the SUSY mass M_{SUSY} in the 200-1000 GeV range. Through all this analysis, we have required compatibility with both the present experimental upper bound for this decay and with neutrino data for masses and oscillations.

We have presented a full computation of $\text{BR}(\tau \rightarrow \mu f_0(980))$ that includes the complete one-loop SUSY diagrams with charginos, neutralinos, sleptons and sneutrinos contributing in the loops to the relevant effective LFV $\tau \mu H$ vertex. We have also taken into account the two kind of Higgs-mediated diagrams, with h^0 and H^0 in the internal propagator connecting the LFV vertex with the final quark-antiquark pairs. On the other hand, and in order to

provide predictions for the final meson $f_0(980)$, we have performed the hadronization of the quark bilinears by means of the standard techniques in χ PT and $R\chi$ T. We have shown that in this chiral approach, the Higgs coupling to the $f_0(980)$ is dominated by its strange quark component. The leading term in this coupling is proportional to m_K^2 , which is a consequence of the Gell-Mann–Oakes–Renner mass relation ($B_0 m_s = m_K^2 - 1/2 m_\pi^2$), and the fact that the Higgs coupling to the strange quark is proportional to m_s . On the other hand, the $H^0 - f_0$ coupling is dominant over the $h^0 - f_0$ coupling since the first one goes approximately as $\tan\beta$ in the large $\tan\beta$ limit (due again to this behaviour of the Hss coupling), whereas the second one is suppressed in this limit.

We have analysed in full detail the dependence of $\text{BR}(\tau \rightarrow \mu f_0(980))$ with all the parameters defining the two constrained SUSY-seesaw scenarios and we have extracted from this analysis which are the relevant ones. Regarding the heavy neutrino sector, and for the most BAU favorable scenario of hierarchical heavy neutrinos, the most relevant parameters are the heaviest neutrino mass, m_{N_3} and the $\theta_{1,2}$ angles. Concerning the SUSY and Higgs sectors the most relevant parameters are the SUSY masses, driven by M_{SUSY} , the CP-even Higgs boson mass, m_{H^0} , and $\tan\beta$.

In the numerical predictions, we have found much larger rates in the NUHM-seesaw than in the CMSSM-seesaw scenarios, due mainly to the lighter Higgs mass m_{H^0} found in the first scheme. Indeed, it is just in the NUHM-seesaw case where the predictions for $\text{BR}(\tau \rightarrow \mu f_0(980))$ can reach the present experimental sensitivity. We have shown, that in order to get values of $\text{BR}(\tau \rightarrow \mu f_0(980))$ at the $10^{-8} - 10^{-7}$ level one needs large values for the relevant parameters, namely, $m_{N_3} \sim 10^{14} - 10^{15}$ GeV, $|\theta_{1,2}| \sim 2 - 3$, $\pm \arg(\theta_{1,2}) \sim \pi/4 - 3\pi/4$, $\tan\beta \sim 50 - 60$ and $m_{H^0} \sim 100 - 200$ GeV.

In addition to the full results, we have provided an approximate simple formula for $\text{BR}(\tau \rightarrow \mu f_0(980))$ which has been obtained in the large M_{SUSY} and large $\tan\beta$ limit, and with the MI approximation for the relevant LFV parameter δ_{32} . Furthermore, we have shown in this work that this approximate result agrees pretty well with the full result in practically all the explored parameter space. The main basic features of the full predicted rates are very well reproduced by the simple formula in (23), which summarizes the fast growing with $\tan\beta$, going as $(\tan\beta)^6$, with $1/m_{H^0}$, going as $(1/m_{H^0})^4$, and being approximately constant with M_{SUSY} . The dependence with m_{N_3} and $\theta_{1,2}$ goes via the δ_{32} parameter, and it is the m_{N_3} which dominates the rates, growing as $\text{BR} \sim |m_{N_3} \log m_{N_3}|^2$.

The most important conclusion from this work, as illustrated in Figs. 7 and 8, is that the LFV tau decay $\tau \rightarrow \mu f_0(980)$ is indeed sensitive to the Higgs sector of the NUHM-seesaw models. Concretely, it is mostly sensitive to the CP-even Higgs boson H^0 , and therefore it

complements very nicely the previous searches via the $\tau \rightarrow \mu\eta$ decay which is sensitive to the CP-odd Higgs boson A^0 . These two channels together with the leptonic $\tau \rightarrow 3\mu$ decay are undoubtedly the most competitive LFV tau decays where to look for indirect Higgs signals. As a final product of our analysis we have extracted some excluded areas in the parameter space of these models by using our approximate formula. The sensitivity found here to the Higgs sector will presumably improve in the future if the experimental reach increases up to 10^{-10} , as it seems to be the case in the future SuperB and flavour factories.

Acknowledgments

M.J.Herrero wishes to thank Simon Eidelman for his encouragement to make this work and for interesting discussions on LFV. This work has been supported in part by the EU MRTN-CT-2006-035482 (FLAVIANet), by MEC (Spain) under grants FPA2006-05423 and FPA2007-60323, by Generalitat Valenciana under the excellence grant PROMETEO/2008/069, by Comunidad de Madrid under HEPHACOS project and by the Spanish Consolider-Ingenio 2010 Programme CPAN (CSD2007-00042). A.M.Rodriguez-Sanchez acknowledges MEC for her FPU fellowship (AP2006-02535).

References

- [1] F. Borzumati and A. Masiero, Phys. Rev. Lett. **57** (1986) 961.
- [2] J. Hisano, T. Moroi, K. Tobe, M. Yamaguchi and T. Yanagida, Phys. Lett. B **357** (1995) 579 [arXiv:hep-ph/9501407];
- [3] J. Hisano, T. Moroi, K. Tobe and M. Yamaguchi, Phys. Rev. D **53** (1996) 2442 [arXiv:hep-ph/9510309].
- [4] J. Hisano and D. Nomura, Phys. Rev. D **59** (1999) 116005 [arXiv:hep-ph/9810479].
- [5] Y. Kuno and Y. Okada, Rev. Mod. Phys. **73** (2001) 151 [arXiv:hep-ph/9909265].
- [6] J. A. Casas and A. Ibarra, Nucl. Phys. B **618** (2001) 171 [arXiv:hep-ph/0103065].
- [7] P. Minkowski, Phys. Lett. B **67** (1977) 421; M. Gell-Mann, P. Ramond and R. Slansky, in *Complex Spinors and Unified Theories* eds. P. Van. Nieuwenhuizen and D. Z. Freedman, *Supergravity* (North-Holland, Amsterdam, 1979), p.315 [Print-80-0576 (CERN)]; T. Yanagida, in *Proceedings of the Workshop on the Unified Theory and the Baryon Number in the Universe*, eds. O. Sawada and A. Sugamoto (KEK, Tsukuba, 1979),

- p.95; S. L. Glashow, in *Quarks and Leptons*, eds. M. Lévy et al. (Plenum Press, New York, 1980), p.687; R. N. Mohapatra and G. Senjanović, Phys. Rev. Lett. **44** (1980) 912.
- [8] K. S. Babu and C. Kolda, Phys. Rev. Lett. **89** (2002) 241802 [arXiv:hep-ph/0206310].
 - [9] M. Sher, Phys. Rev. D **66** (2002) 057301 [arXiv:hep-ph/0207136].
 - [10] A. Dedes, J. R. Ellis and M. Raidal, Phys. Lett. B **549** (2002) 159 [arXiv:hep-ph/0209207].
 - [11] R. Kitano, M. Koike, S. Komine and Y. Okada, Phys. Lett. B **575** (2003) 300 [arXiv:hep-ph/0308021].
 - [12] A. Brignole and A. Rossi, Phys. Lett. B **566** (2003) 217 [arXiv:hep-ph/0304081];
 - [13] A. Brignole and A. Rossi, Nucl. Phys. B **701** (2004) 3 [arXiv:hep-ph/0404211].
 - [14] E. Arganda, A. M. Curiel, M. J. Herrero and D. Temes, Phys. Rev. D **71** (2005) 035011 [arXiv:hep-ph/0407302].
 - [15] P. Paradisi, JHEP **0510** (2005) 006 [arXiv:hep-ph/0505046].
 - [16] E. Arganda and M. J. Herrero, Phys. Rev. D **73** (2006) 055003 [arXiv:hep-ph/0510405].
 - [17] P. Paradisi, JHEP **0602** (2006) 050 [arXiv:hep-ph/0508054].
 - [18] C. H. Chen and C. Q. Geng, Phys. Rev. D **74** (2006) 035010 [arXiv:hep-ph/0605299].
 - [19] S. Antusch, E. Arganda, M. J. Herrero and A. M. Teixeira, JHEP **0611** (2006) 090 [arXiv:hep-ph/0607263].
 - [20] E. Arganda, M. J. Herrero and A. M. Teixeira, JHEP **0710** (2007) 104 [arXiv:0707.2955 [hep-ph]].
 - [21] E. Arganda, M. J. Herrero and J. Portolés, JHEP **0806** (2008) 079 [arXiv:0803.2039 [hep-ph]].
 - [22] T. Fukuyama, A. Ilakovac and T. Kikuchi, Eur. Phys. J. C **56** (2008) 125 [arXiv:hep-ph/0506295].
 - [23] E. Arganda, M. Herrero, J. Portoles, A. Rodriguez-Sanchez and A. M. Teixeira, arXiv:0812.2692 [hep-ph].

- [24] C. Amsler *et al.* [Particle Data Group], Phys. Lett. B **667** (2008) 1.
- [25] M. L. Brooks *et al.* [MEGA Collaboration], Phys. Rev. Lett. **83** (1999) 1521 [arXiv:hep-ex/9905013].
- [26] S. Ritt [MEG Collaboration], Nucl. Phys. Proc. Suppl. **162** (2006) 279.
- [27] C. Dohmen *et al.* [SINDRUM II Collaboration.], Phys. Lett. B **317**, 631 (1993).
- [28] W. Bertl *et al.* [SINDRUM II Collaboration], Eur. Phys. J. C **47**, 337 (2006).
- [29] U. Bellgardt *et al.* [SINDRUM Collaboration], Nucl. Phys. B **299**, 1 (1988).
- [30] B. Aubert *et al.* [BABAR Collaboration], Phys. Rev. Lett. **95** (2005) 041802 [arXiv:hep-ex/0502032].
- [31] K. Abe *et al.* [Belle Collaboration], arXiv:hep-ex/0609049.
- [32] K. Hayasaka *et al.* [Belle Collaboration], arXiv:0705.0650 [hep-ex].
- [33] S. Banerjee, Nucl. Phys. Proc. Suppl. **169** (2007) 199 [arXiv:hep-ex/0702017].
- [34] Y. Miyazaki *et al.* [Belle Collaboration], arXiv:0711.2189 [hep-ex].
- [35] B. Aubert *et al.* [BABAR Collaboration], Phys. Rev. Lett. **99** (2007) 251803 [arXiv:0708.3650 [hep-ex]].
- [36] Y. Yusa *et al.* [BELLE Collaboration], Phys. Lett. B **640** (2006) 138 [arXiv:hep-ex/0603036].
- [37] K. Abe *et al.* [Belle Collaboration], arXiv:hep-ex/0609013.
- [38] B. Aubert *et al.* [BABAR Collaboration], Phys. Rev. Lett. **98** (2007) 061803 [arXiv:hep-ex/0610067].
- [39] Y. Miyazaki *et al.* [BELLE Collaboration], Phys. Lett. B **648** (2007) 341 [arXiv:hep-ex/0703009].
- [40] Y. Miyazaki, arXiv:0810.3519 [hep-ex].
- [41] S. Weinberg, PhysicaA **96** (1979) 327;
- [42] J. Gasser and H. Leutwyler, Annals Phys. **158** (1984) 142.

- [43] J. Gasser and H. Leutwyler, Nucl. Phys. B **250** (1985) 465.
- [44] G. Ecker, J. Gasser, A. Pich and E. de Rafael, Nucl. Phys. B **321** (1989) 311;
J. F. Donoghue, C. Ramírez and G. Valencia, Phys. Rev. D **39** (1989) 1947.
- [45] G. Ecker, J. Gasser, H. Leutwyler, A. Pich and E. de Rafael, Phys. Lett. B **223** (1989) 425;
- [46] A. Pich, in: R.F. Lebed (Ed.), Phenomenology of Large- N_C QCD, World Scientific, Singapore, 2002, arXiv:hep-ph/0205030.
- [47] V. Cirigliano, G. Ecker, H. Neufeld and A. Pich, JHEP **0306** (2003) 012 [arXiv:hep-ph/0305311].
- [48] V. Cirigliano, G. Ecker, M. Eidemueller, R. Kaiser, A. Pich and J. Portolés, Nucl. Phys. B **753** (2006) 139 [arXiv:hep-ph/0603205].
- [49] For a review see, for instance,
G. L. Kane, C. F. Kolda, L. Roszkowski and J. D. Wells, Phys. Rev. D **49** (1994) 6173 [arXiv:hep-ph/9312272].
- [50] For a review see, for instance,
J. R. Ellis, T. Falk, K. A. Olive and Y. Santoso, Nucl. Phys. B **652** (2003) 259 [arXiv:hep-ph/0210205];
- [51] B. Pontecorvo, Sov. Phys. JETP **6** (1957) 429 [Zh. Eksp. Teor. Fiz. **33** (1957) 549]; Sov. Phys. JETP **7** (1958) 172 [Zh. Eksp. Teor. Fiz. **34** (1957) 247].
- [52] Z. Maki, M. Nakagawa and S. Sakata, Prog. Theor. Phys. **28** (1962) 870.
- [53] W. Porod, Comput. Phys. Commun. **153** (2003) 275 [arXiv:hep-ph/0301101].